nature portfolio

https://doi.org/10.1038/s41596-022-00714-6

Supplementary information

Utilizing Skyline to analyze lipidomics data containing liquid chromatography, ion mobility spectrometry and mass spectrometry dimensions

In the format provided by the authors and unedited

Supplementary Information for

Utilizing Skyline to Analyze Lipidomics Data Containing Liquid Chromatography, Ion Mobility Spectrometry and Mass Spectrometry Dimensions

Kaylie I. Kirkwood[1], Brian S. Pratt[2], Nicholas Shulman[2], Kaipo Tamura[2], Michael J. MacCoss[2], Brendan X. MacLean[2], Erin S. Baker[1,3,*]

[1]*Department of Chemistry, North Carolina State University, Raleigh, NC*
[2]*Department of Genome Sciences, University of Washington, Seattle, WA*
[3]*Comparative Medicine Institute, North Carolina State University, Raleigh, NC*

***Corresponding author**: Erin Baker, ebaker@ncsu.edu

Supplementary Methods

Plasma Lipid Extraction

Lipid extractions for each plasma dataset were performed using a modified Folch extraction[1]. First, 600 µL of 2:1 -20°C chloroform/methanol was added to 50 µL of plasma and vortexed for 30 s. Then 150 µL of water was added and vortexed for 30 s to induce phase separation. The samples sat for 5 min at room temperature then were centrifuged at 10,000xg for 10 min at 4°C. The samples were then placed on ice to prevent diffusion then an equal volume of the bottom lipid layer was removed and the solvent was evaporated using a SpeedVac. For long-term storage, the lipid extracts were reconstituted in 300 µL of 2:1 chloroform/methanol and stored at -20°C. Solvent was evaporated prior to analysis using a SpeedVac and reconstituted in 10 µL of chloroform, then 190 µL of methanol was added. Note that following this extraction method is not required to follow the protocol. It is recommended to use a smaller volume of plasma to conserve samples and prevent column overloading.

LC Method

Either a Waters Acquity UPLC H-Class system or an Agilent 1260 or 1290 Infinity HPLC were used. Sample volumes of 10 µL were injected onto a reversed phase Waters CSH column (3.0 mm x 150 mm x 1.7 µm particle size). Lipids were separated over a 34 min gradient with a mobile phase A of 10 mM ammonium acetate in 40:60 acetonitrile/water and a mobile phase B of 10 mM ammonium acetate in 10:90 acetonitrile/isopropanol at a flow rate of 250 µL/min. The column was

washed for 4 min. The gradient and column wash and equilibration steps are provided in **Supplementary Table 3**.

Supplementary Table 3: LC gradient and column wash steps

Step	Time	% A	% B	Flow rate (µL/min)
Gradient	0	60	40	250
Gradient	2	50	50	250
Gradient	3	40	60	250
Gradient	12	30	70	250
Gradient	15	25	75	250
Gradient	17	22	78	250
Gradient	19	15	85	250
Gradient	22	8	92	250
Gradient	25	1	99	250
Gradient	34	1	99	250
Wash	34.5	60	40	300
Wash	35	1	99	300
Wash	35.5	1	99	300
Equilibration	36	60	40	305
Equilibration	37	60	40	300
Equilibration	38	60	40	250

IMS-CID-MS Method

The Agilent 6560 IM-qTOF-MS platform was utilized (Santa Clara, CA) with the commercial gas kit (Alternate Gas Kit, Agilent), a precision flow controller (640B, MKS Instruments) and the Agilent Jet Stream ESI source. IMS-MS data was collected in both positive and negative ionization modes from m/z 50-1700 with a cycle time of 1 s/spectra, an IM trap fill time of 10000 µs and trap release time of 400 µs. Lipids were fragmented via CID using a DIA All Ions method and a ramped collision energy (**Supplementary Table 4**).

Supplementary Table 4: Collision energy scheme

Drift Time	Collision Energy
0	10
15	14
19	27
25	45
40	52
50	58

LC-IMS-CID-MS data was single-field calibrated using Agilent Tune Mix and IM-MS Browser software prior to import.

Supplementary Figures and Tables

Supplementary Table 5: Confidence criteria for lipid inclusion in library

Criteria	Threshold
Lipid presence	>1 sample
Mass error	≤5 ppm for precursors, 10 ppm for fragments
Fragments	Drift-aligned and match literature or in silico spectra
Retention time	Within class-specific window
CCS	Within 2% of database value (if present)
CCS vs. m/z	Fits class-specific trendline

Supplementary Figure 1: Protocol step 2

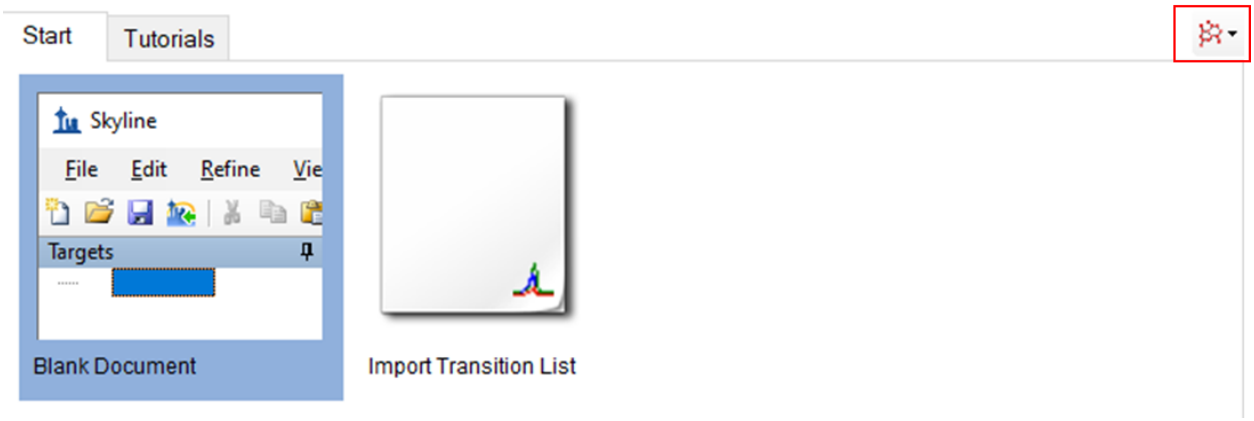

Supplementary Figure 1. Screenshot corresponding to step 2 of the protocol where the small molecule interface (highlighted in a red box) is selected on the start page of Skyline.

Supplementary Figure 2: Protocol step 3B

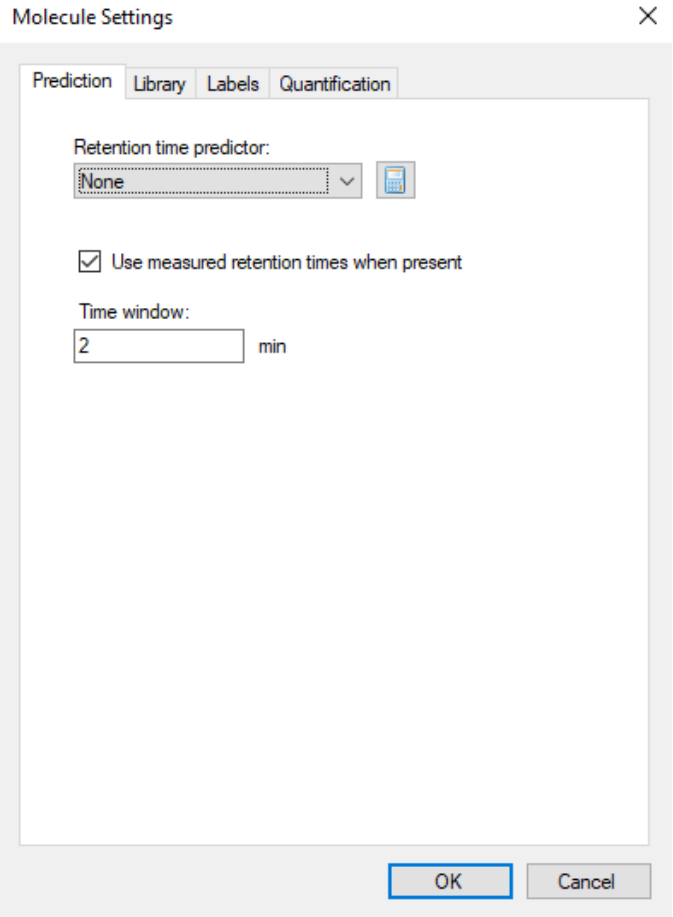

Supplementary Figure 2. Screenshot corresponding to step 3B (I) of the protocol to remove the iRT calculator if it is not applicable to your LC method.

Supplementary Figure 3: Protocol steps 5-8

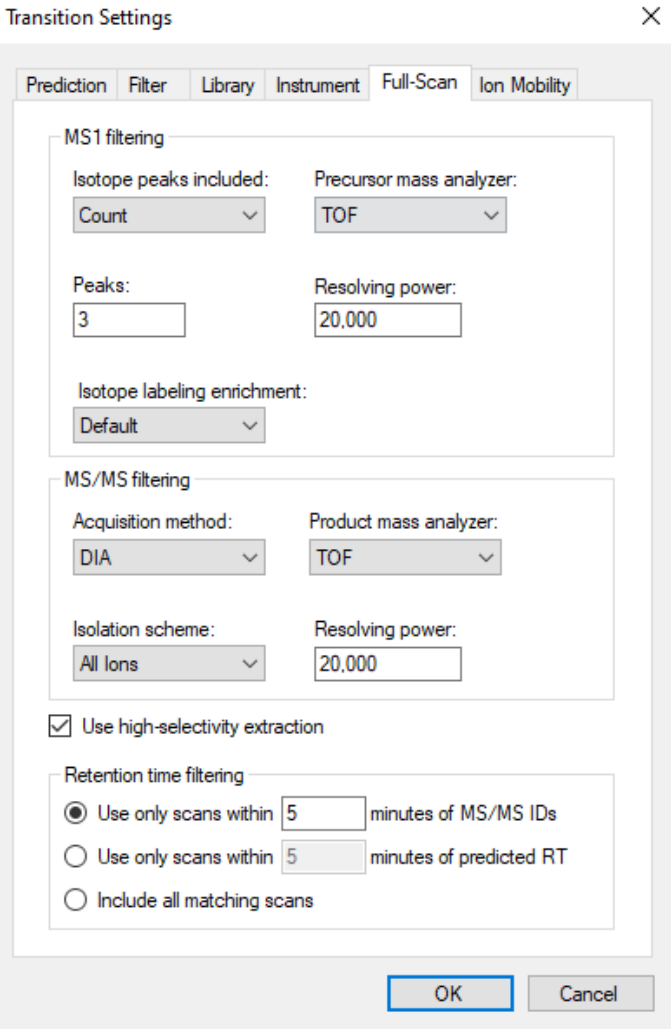

Supplementary Figure 3. Screenshot corresponding to steps 5-8 of the protocol which are optional steps to edit the MS settings if different mass spectrometry platforms were used. The settings saved to the library files and shown here are appropriate for a TOF instrument with a resolving power of 20,000-30,000 using a data-independent acquisition method with an all ions fragmentation method.

Supplementary Figure 4: Protocol steps 9-10

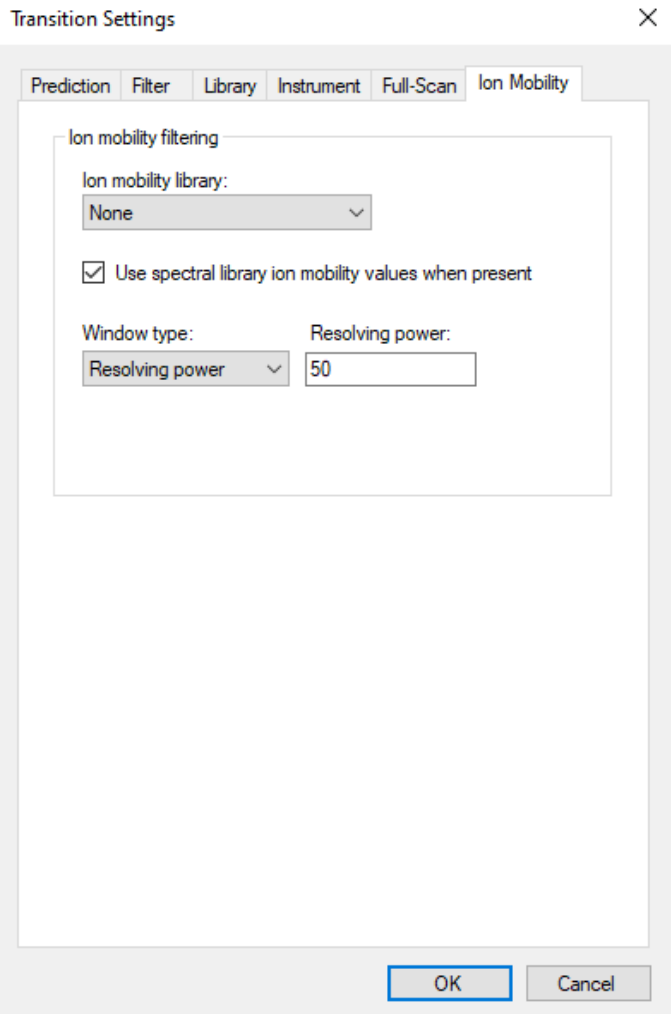

Supplementary Figure 4. Screenshot corresponding to steps 9-10 of the protocol which are optional steps to edit the IMS settings if different ion mobility spectrometry platforms were used. The settings saved to the library files and shown here are appropriate for a DTIMS instrument with a resolving power of 50.

Supplementary Figure 5: Protocol step 12

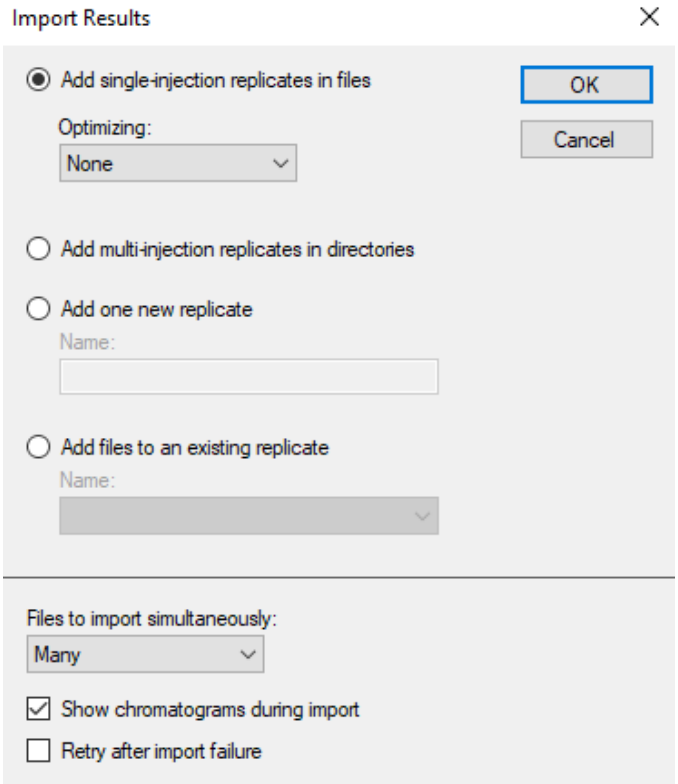

Supplementary Figure 5. Screenshot corresponding to step 12 of the protocol to import results. Here, 'Files to import simultaneously' is set to 'Many' and 'Show chromatograms during import' is checked, however the default settings may vary and should not impact the data import.

Supplementary Figure 6: Protocol steps 14 and 32

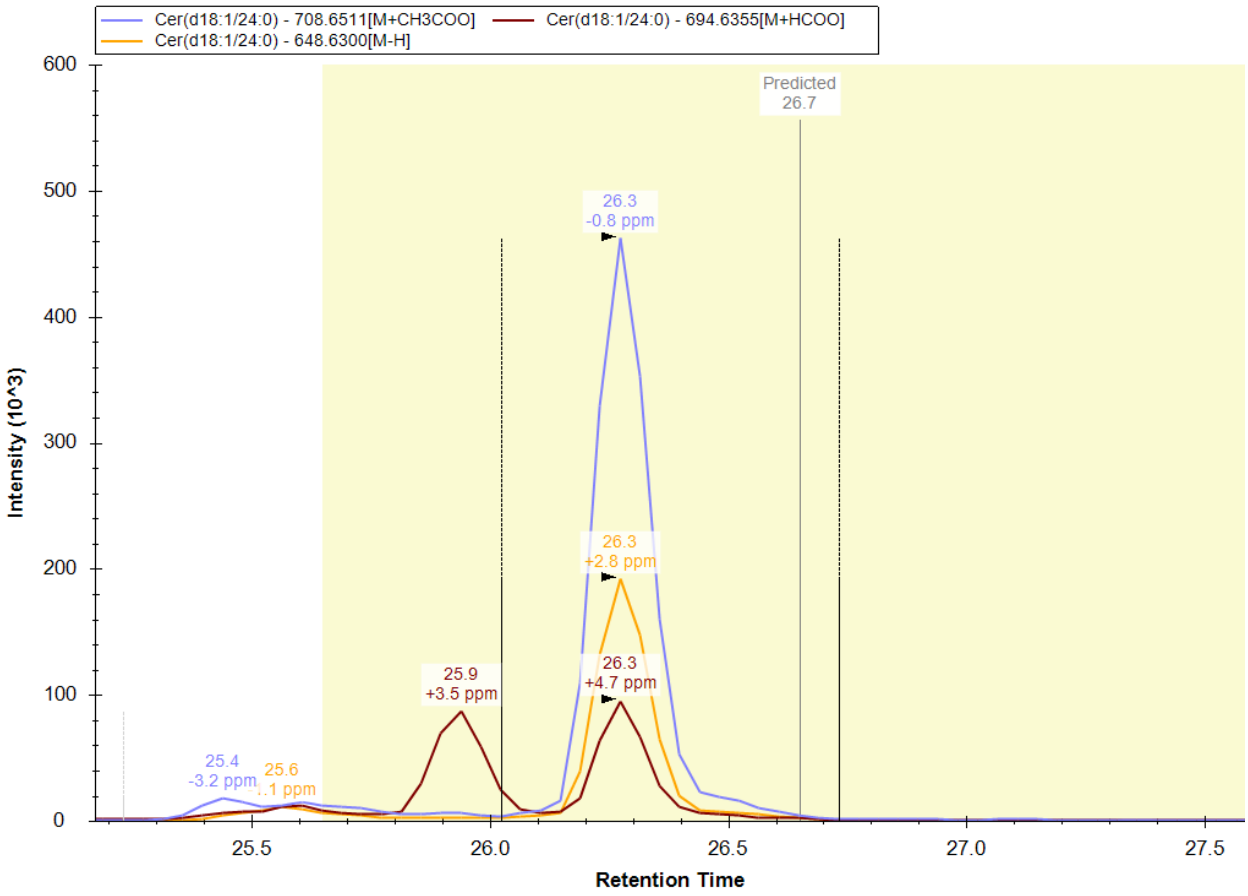

Supplementary Figure 6. Screenshot corresponding to steps 14 and 32 of the protocol displaying co-elution of the three adducts for the iRT calibrant lipid Cer(d18:1/24:0) in negative ionization mode. The retention time is predicted at 26.7 min, however this may shift as more iRT calibrant lipid peaks are selected. The mass error of each precursor is displayed above the peak apex. As displayed in the legend, the gray trace corresponds to the acetate-adducted species, the yellow trace corresponds to the deprotonated species, and the brown trace corresponds to the formate-adducted species. Each precursor and its corresponding fragments can be further inspected individually.

Supplementary Figure 7: Protocol steps 15-16 and 33-34

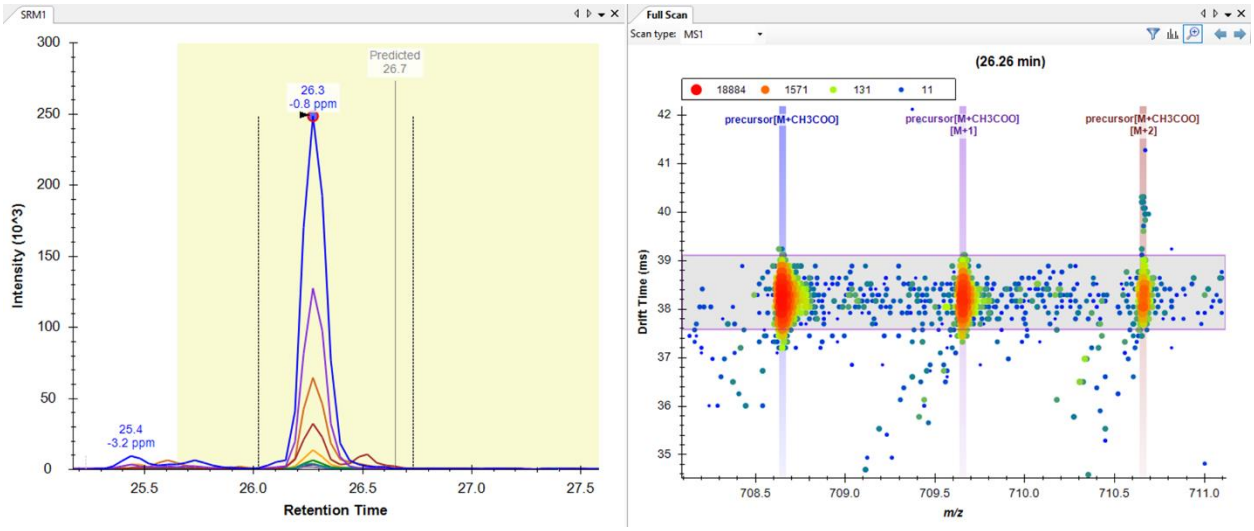

Supplementary Figure 7. Screenshot corresponding to steps 15-16 and 33-34 of the protocol where the precursor peak apex of a candidate peak for the iRT calibrant lipid Cer(d18:1/24:0) $[M+CH_3COO]^-$ is selected, as shown by Skyline with a red circle, to view the 2D MS spectrum.

Supplementary Figure 8: Protocol steps 17 and 35

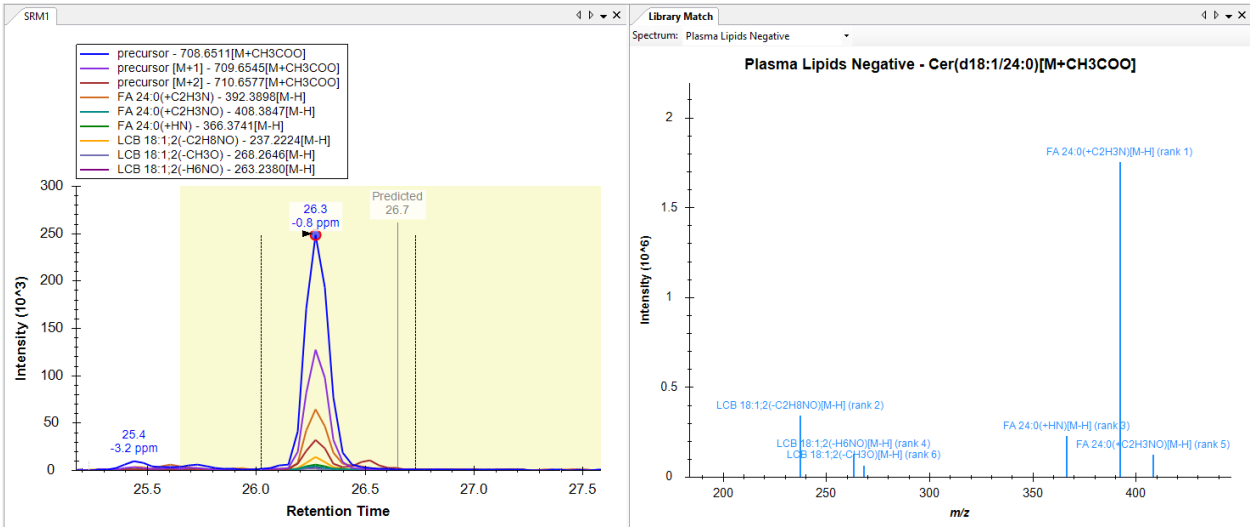

Supplementary Figure 8. Screenshot corresponding to steps 17 and 35 of the protocol where the spectral library match for Cer(d18:1/24:0) $[M+CH_3COO]^-$ is displayed next to the experimental chromatogram for the same lipid. A legend is displayed in the chromatogram window to identify the corresponding fragments, which can also be individually highlighted when selected in the 'Targets' pane.

Supplementary Figure 9: Protocol steps 30 and 50

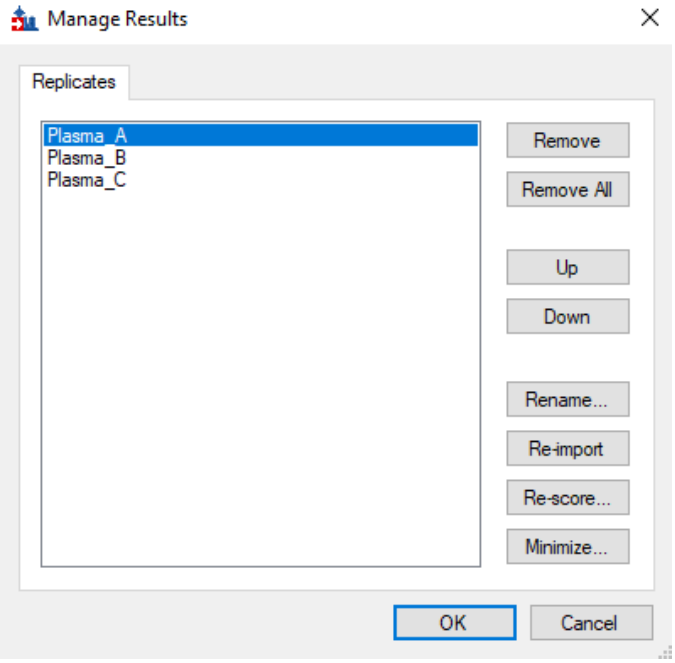

Supplementary Figure 9. Screenshot corresponding to steps 30 and 50 of the protocol in order to re-import/extract data after making changes to the target list.

Supplementary Figure 10: Protocol step 31

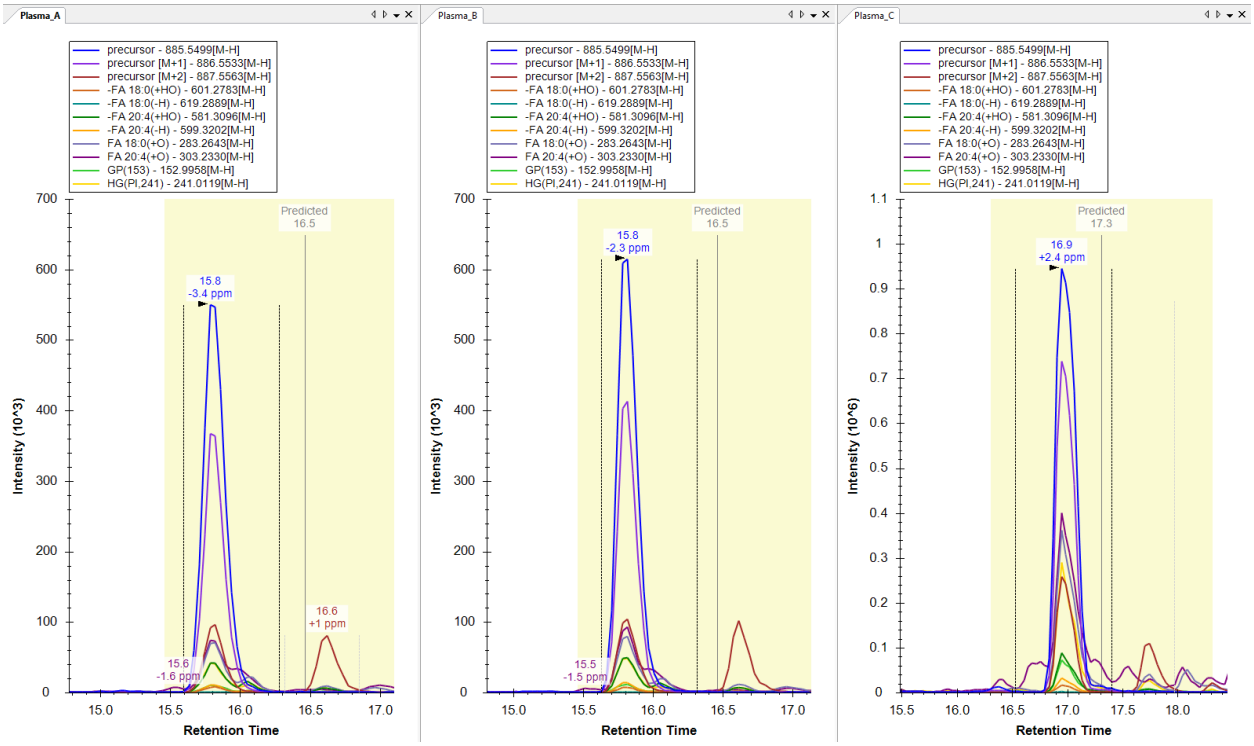

Supplementary Figure 10. Screenshot corresponding to step 31 of the protocol where a 'Tiled' view is selected to view 3 samples simultaneously. In this example, the lipid PI(18:0_20:4) $[M-H]^-$ is in view. Note that the abundances of the fragments relative to the precursor for this lipid in Plasma_C are higher than those in Plasma_A and Plasma_B due to signal saturation in Plasma_C, as these samples were not from the same sample set and Plasma_C was collected in a different laboratory.

Supplementary Figure 11: Protocol step 36

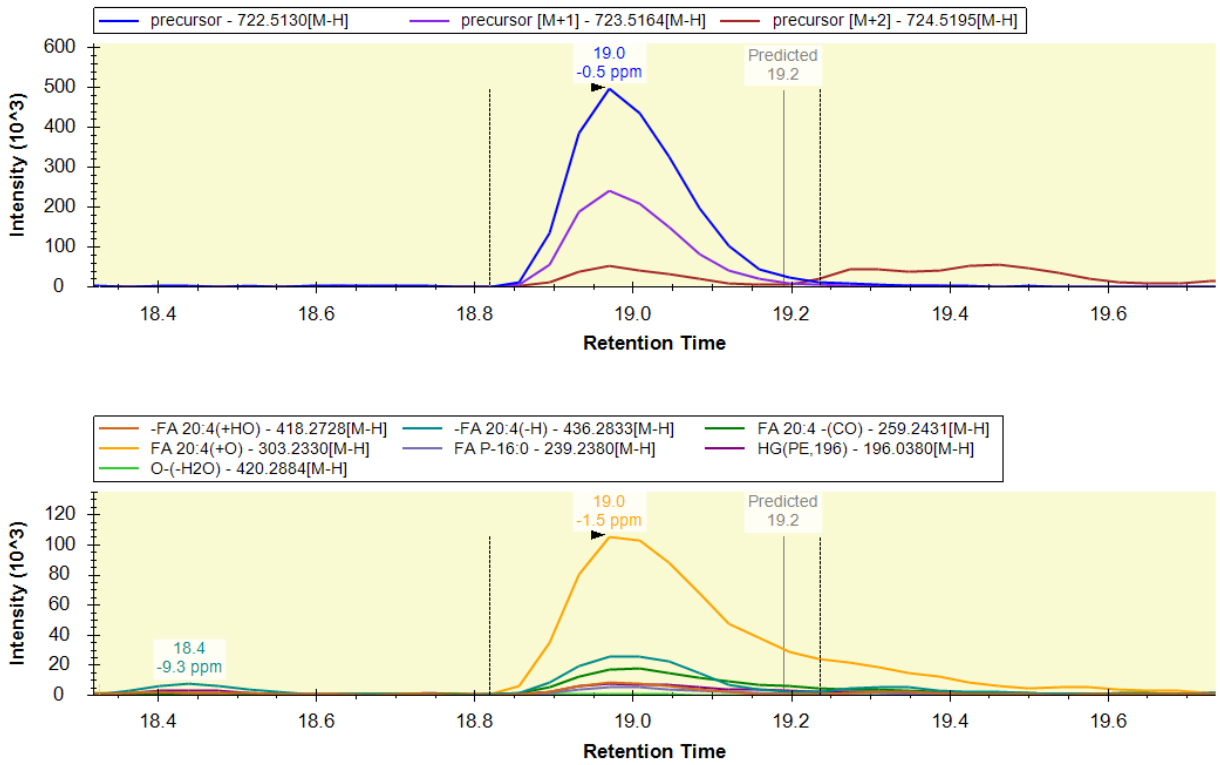

Supplementary Figure 11. Screenshot corresponding to step 36 of the protocol where the precursor (top) and fragment (bottom) chromatograms are split into different panes with different y-axis scales. In this example, the lipid PE(P-16:0/20:4) $[M-H]^-$ is in view.

Supplementary Figure 12: Protocol step 47

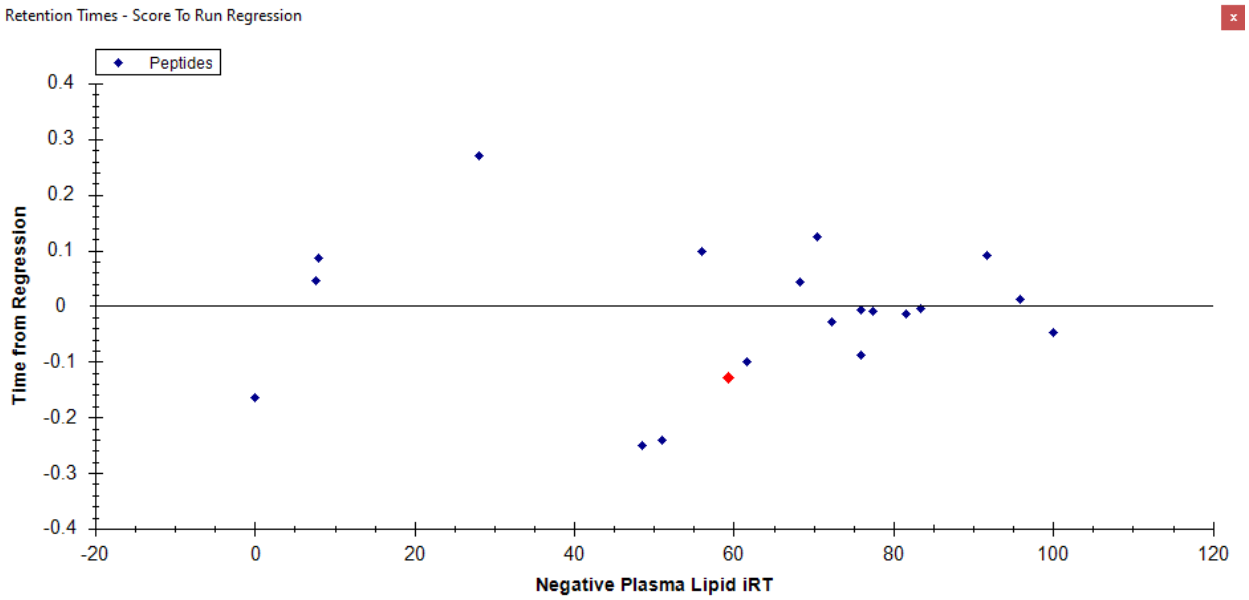

Supplementary Figure 12. Screenshot corresponding to step 47 of the protocol where the residuals are plotted in the 'Retention Times – Scores to Run Regression' window to evaluate the iRT prediction performance. In this example, only the 20 calibrant lipids are shown for clarity as opposed to the entire library.

Supplementary Figure 13: Protocol step 49A

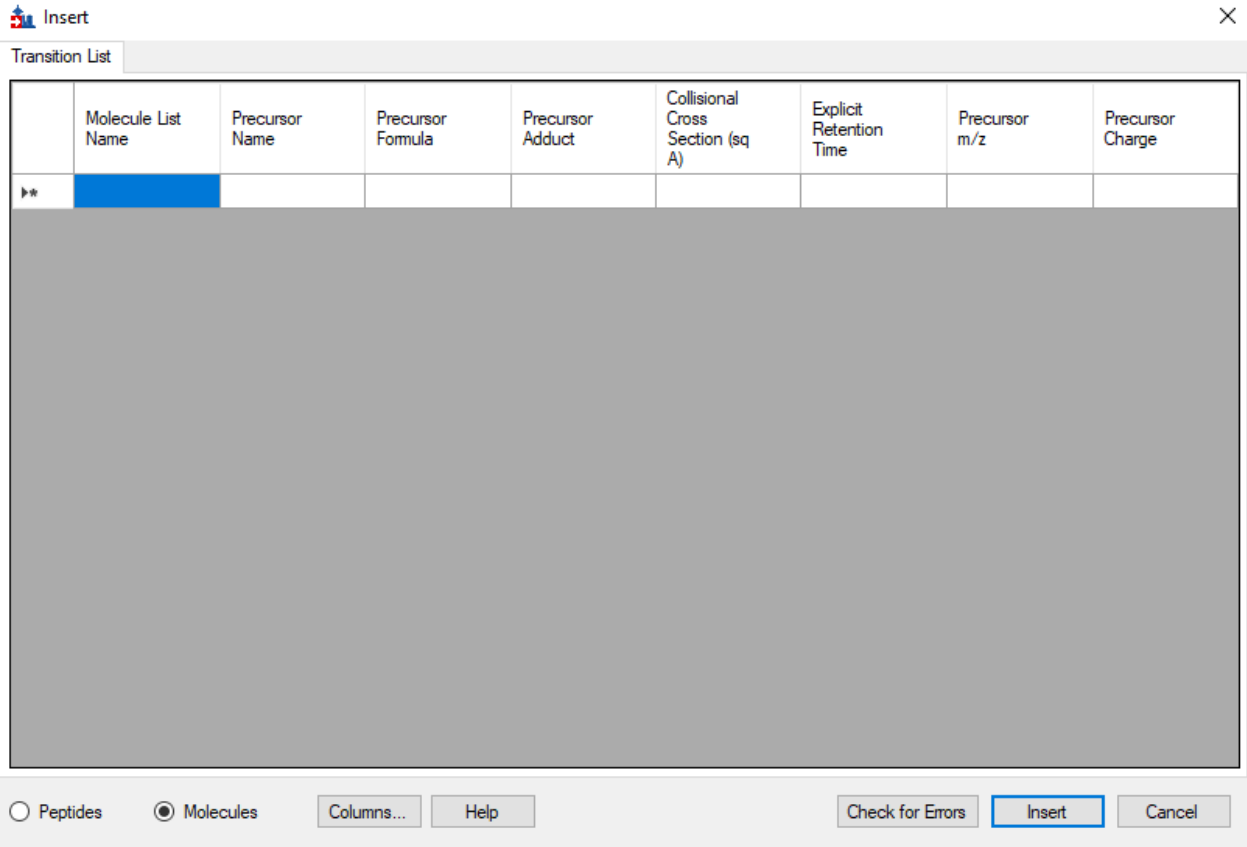

Supplementary Figure 13. Screenshot corresponding to step 49A of the protocol giving an example of potential columns of interest to add when inserting a transition list for additional lipids beyond the library.

Supplementary Figure 14: Protocol steps 53-56

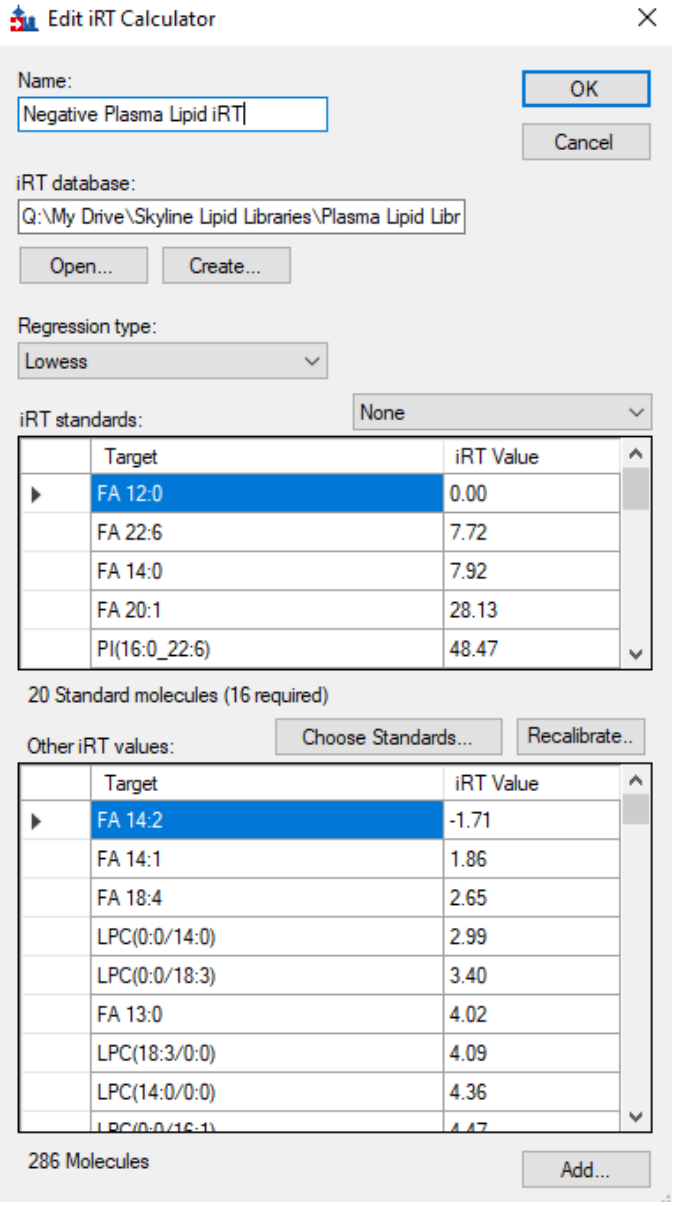

Supplementary Figure 14. Screenshot corresponding to steps 53-56 of the protocol to add additional targets to the iRT calculator or choose different standards (calibrant lipids) in the 'Edit iRT Calculator' window.

Supplementary Figure 15: Protocol steps 58 and 62

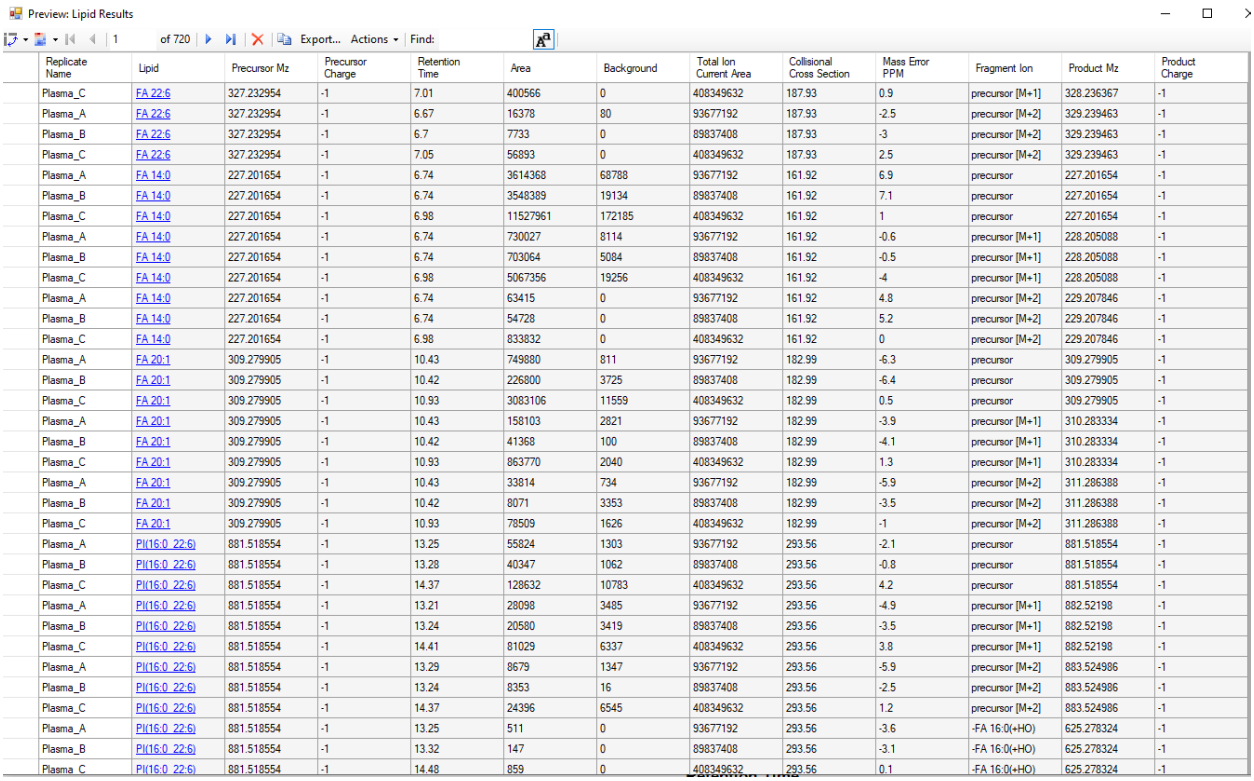

Replicate Name	Lipid	Precursor Mz	Precursor Charge	Retention Time	Area	Background	Total Ion Current Area	Collisional Cross Section	Mass Error PPM	Fragment Ion	Product Mz	Product Charge
Plasma_C	FA 22:6	327.232954	-1	7.01	400566	0	408349632	187.93	0.9	precursor [M+1]	328.236367	-1
Plasma_A	FA 22:6	327.232954	-1	6.67	16378	80	93677192	187.93	-2.5	precursor [M+2]	329.239463	-1
Plasma_B	FA 22:6	327.232954	-1	6.7	7733	0	89837408	187.93	-3	precursor [M+2]	329.239463	-1
Plasma_C	FA 22:6	327.232954	-1	7.05	56893	0	408349632	187.93	2.5	precursor [M+2]	329.239463	-1
Plasma_A	FA 14:0	227.201654	-1	6.74	3614368	68788	93677192	161.92	6.9	precursor	227.201654	-1
Plasma_B	FA 14:0	227.201654	-1	6.74	3548389	19134	89837408	161.92	7.1	precursor	227.201654	-1
Plasma_C	FA 14:0	227.201654	-1	6.98	11527961	172185	408349632	161.92	1	precursor	227.201654	-1
Plasma_A	FA 14:0	227.201654	-1	6.74	730027	8114	93677192	161.92	-0.6	precursor [M+1]	228.205088	-1
Plasma_B	FA 14:0	227.201654	-1	6.74	703064	5084	89837408	161.92	-0.5	precursor [M+1]	228.205088	-1
Plasma_C	FA 14:0	227.201654	-1	6.98	5067356	19256	408349632	161.92	-4	precursor [M+1]	228.205088	-1
Plasma_A	FA 14:0	227.201654	-1	6.74	63415	0	93677192	161.92	4.8	precursor [M+2]	229.207846	-1
Plasma_B	FA 14:0	227.201654	-1	6.74	54728	0	89837408	161.92	5.2	precursor [M+2]	229.207846	-1
Plasma_C	FA 14:0	227.201654	-1	6.98	833832	0	408349632	161.92	0	precursor [M+2]	229.207846	-1
Plasma_A	FA 20:1	309.279905	-1	10.43	749880	811	93677192	182.99	-6.3	precursor	309.279905	-1
Plasma_B	FA 20:1	309.279905	-1	10.42	226800	3725	89837408	182.99	-6.4	precursor	309.279905	-1
Plasma_C	FA 20:1	309.279905	-1	10.93	3083106	11559	408349632	182.99	0.5	precursor	309.279905	-1
Plasma_A	FA 20:1	309.279905	-1	10.43	158103	2821	93677192	182.99	-3.9	precursor [M+1]	310.283334	-1
Plasma_B	FA 20:1	309.279905	-1	10.42	41368	100	89837408	182.99	-4.1	precursor [M+1]	310.283334	-1
Plasma_C	FA 20:1	309.279905	-1	10.93	863770	2040	408349632	182.99	1.3	precursor [M+1]	310.283334	-1
Plasma_A	FA 20:1	309.279905	-1	10.43	33814	734	93677192	182.99	-5.9	precursor [M+2]	311.286388	-1
Plasma_B	FA 20:1	309.279905	-1	10.42	8071	3353	89837408	182.99	-3.5	precursor [M+2]	311.286388	-1
Plasma_C	FA 20:1	309.279905	-1	10.93	78509	1626	408349632	182.99	-1	precursor [M+2]	311.286388	-1
Plasma_A	PI(16:0_22:6)	881.518554	-1	13.25	55824	1303	93677192	293.56	-2.1	precursor	881.518554	-1
Plasma_B	PI(16:0_22:6)	881.518554	-1	13.28	40347	1062	89837408	293.56	-0.8	precursor	881.518554	-1
Plasma_C	PI(16:0_22:6)	881.518554	-1	14.37	128632	10783	408349632	293.56	4.2	precursor	881.518554	-1
Plasma_A	PI(16:0_22:6)	881.518554	-1	13.21	28098	3485	93677192	293.56	-4.9	precursor [M+1]	882.52198	-1
Plasma_B	PI(16:0_22:6)	881.518554	-1	13.24	20580	3419	89837408	293.56	-3.5	precursor [M+1]	882.52198	-1
Plasma_C	PI(16:0_22:6)	881.518554	-1	14.41	81029	6337	408349632	293.56	3.8	precursor [M+1]	882.52198	-1
Plasma_A	PI(16:0_22:6)	881.518554	-1	13.29	8679	1347	93677192	293.56	-5.9	precursor [M+2]	883.524986	-1
Plasma_B	PI(16:0_22:6)	881.518554	-1	13.24	8353	16	89837408	293.56	-2.5	precursor [M+2]	883.524986	-1
Plasma_C	PI(16:0_22:6)	881.518554	-1	14.37	24396	6545	408349632	293.56	1.2	precursor [M+2]	883.524986	-1
Plasma_A	PI(16:0_22:6)	881.518554	-1	13.25	511	0	93677192	293.56	-3.6	-FA 16:0(+HO)	625.278324	-1
Plasma_B	PI(16:0_22:6)	881.518554	-1	13.32	147	0	89837408	293.56	-3.1	-FA 16:0(+HO)	625.278324	-1
Plasma_C	PI(16:0_22:6)	881.518554	-1	14.48	859	0	408349632	293.56	0.1	-FA 16:0(+HO)	625.278324	-1

Supplementary Figure 15. Screenshot corresponding to steps 58 and 62 of the protocol of an example report preview. In this example, a custom report was developed which includes replicate (sample) name, lipid name, precursor m/z and charge, retention time, peak area, background signal, total ion current area, CCS, mass error, fragment ion name, and product m/z and charge.

Supplementary Figure 16: Protocol steps 59-60

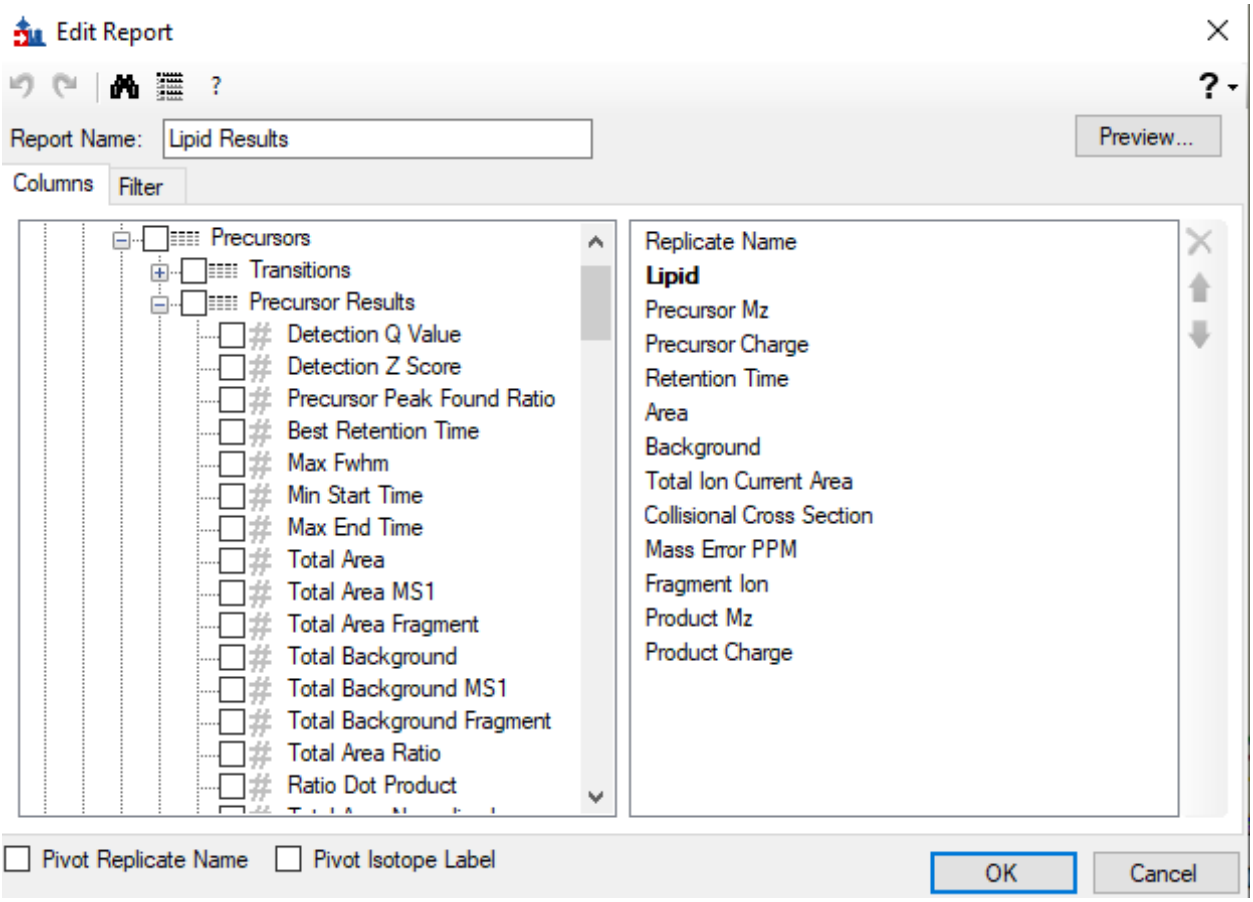

Supplementary Figure 16. Screenshot corresponding to steps 59-60 of the protocol displaying the hierarchical list which can be used to select additional columns or delete/rename existing columns for the exported report. The binocular icon in the top left corner can be used to search for specific terms.

Supplementary Figure 17: Co-eluting isobaric species

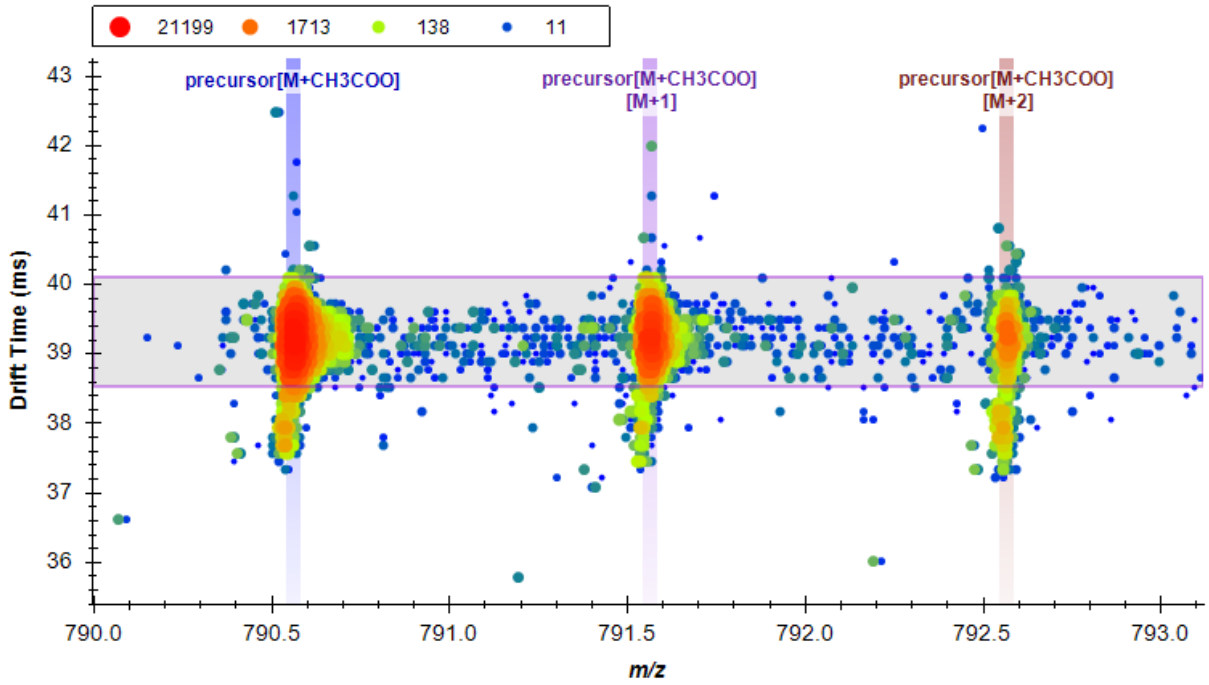

Supplementary Figure 17. Example of MS1 drift time filtering of interferences. In this case, an isobar of PC(16:0_16:1) $[M+CH_3COO]^-$ is co-eluting in the LC dimension and would contribute to the extracted precursor ion intensities if drift time filtering was not utilized. However, these isobars are well-separated in the IMS drift time dimension, thus the interference is filtered out.

References

1. Folch, J.; Lees, M.; Sloane Stanley, G. H., A simple method for the isolation and purification of total lipides from animal tissues. *J Biol Chem* **1957,** *226* (1), 497-509.